PCCP

Does a Halogen Bond Require Positive Potential on the Acid and Negative Potential on the Base?

Journal:	*Physical Chemistry Chemical Physics*
Manuscript ID	CP-ART-01-2023-000379.R1
Article Type:	Paper
Date Submitted by the Author:	17-Feb-2023
Complete List of Authors:	Scheiner, Steve; Utah State University, Department of Chemistry and Biochemistry

Does a Halogen Bond Require Positive Potential on the Acid and Negative Potential on the Base?

Steve Scheiner*
Department of Chemistry and Biochemistry
Utah State University
Logan, Utah 84322-0300

email: steve.scheiner@usu.edu

Abstract

It is usually expected that formation of a halogen bond (XB) requires that a region of positive electrostatic potential associated with a σ or π-hole on the Lewis acid will interact with the negative potential of the base, either a lone pair or π-bond region. Quantum calculations of model systems suggest this not to be necessary. The placement of electron-withdrawing substituents on the base can reverse the sign of the potential in its lone pair or π-bond region to positive, and this base can nonetheless engage in a XB with the positive σ-hole of a Lewis acid. The reverse scenario is also possible in certain circumstances, as a negatively charged σ-hole can form a XB with the negative lone pair region of a base. Despite these classical Coulombic repulsions, the overall electrostatic interaction is attractive in these XBs, albeit only weakly so. The strengths of these bonds are surprisingly insensitive to changes in the partner molecule. For example, even a wide range in the depth of the σ-hole of the approaching acid yields only a minimal change in the strength of the XB to a base with a positive potential.

keywords: noncovalent bond; electrostatic potential; energy decomposition; QTAIM; NBO

INTRODUCTION

A century of study of the H-bond has attributed its stability to several factors [1-7]. Generally considered the most important of these is an electrostatic attraction between the partial positive charge of the bridging proton and the negative segment of the base that coincides with its lone pair or its π-electron region. Other important contributors to the H-bond are thought to be a charge transfer from the base to the σ*(RH) antibonding orbital of the proton donor molecule, as well as attractive dispersive forces. The halogen bond (XB) is quite similar to the H-bond except that the bridging H is replaced by any of the various halogen atoms. As study of the XB has ramped up over recent years it has come to be understood that very similar factors contribute to its stability [8-17]. The primary difference is that the overall positive charge of the bridging H is replaced by a narrower positive region that lies along the extension of the RX covalent bond, known generally as a σ-hole. This polar hole is surrounded by a negative equator that leaves the X atom with an overall negative charge, which tends to make the XB somewhat more directional than a standard HB. It might be added parenthetically that this same concept of σ-holes lying along the extension of a covalent bond applies equally to a number of close cousins of the XB, such as chalcogen, pnicogen, and tetrel bonds, each named according to the column of the periodic table from which the bridging atom is drawn [18-29].

Extensive study of the XB has led to a number of general guidelines concerning its strength. Because of the dominating influence of the Coulombic attraction between the positive and negative regions of the acid and base, respectively, the magnification of the potential of either of these units will typically amplify the XB strength. With specific regard to the acid, the heavier X atoms are more electropositive than their lighter congeners, and more polarizable as well. The order of XB strength therefore typically obeys the order I > Br > Cl which is parallel to the depth of the σ-hole on each of these centers. (F is too electronegative to contain a positive σ-hole so very rarely participates in a XB.) As another factor, any electron-withdrawing substituents on the acid molecule withdraw density from X, thereby accentuating its σ-hole, which ultimately results in a stronger XB. In a similar vein, any qualities of the base that heighten the negative charge of the segment approaching the acid will also act to amplify the XB strength.

The molecular electrostatic potential (MEP) surrounding each molecule is a three-dimensional function with positive and negative regions of varying degree. One could imagine a number of ways in which to summarize its salient characteristics. The most commonly adopted scheme is to consider a surface with a particular density and to present the MEP on this isodensity surface as a color scheme, with red and blue at its two extremes. The MEP will have maxima and minima on this surface, which can be evaluated and are then presented numerically as $V_{max,S}$ and $V_{min,S}$. Of course, there is a good deal of arbitrariness baked into the particular density which is taken for this surface, but the majority of work in the field apply ρ=0.001 au which is thought to very roughly approximate a vdW surface. Regardless of this arbitrariness, the derived values of $V_{max,S}$ and $V_{min,S}$ have proven useful in predicting the relative strengths of various XBs, and their product correlates fairly well with XB energetics in certain situations.

It is commonly assumed that the formation of a XB is predicated on the presence of a positive σ-hole of substantial depth on the Lewis acid, coupled with the negative potential on the region of the base with which it comes into contact. The basis of this presumption is that this pairing of opposite charges is necessary to generate the required electrostatic attraction between the two entities. But this supposed requirement has never been thoroughly tested. One can imagine a scenario wherein the charge transfer between the two molecules is sufficient to compensate for the lack of a strong electrostatic attraction. Indeed, when coupled with dispersion, it is conceivable that these attractive components might overcome a mild electrostatic repulsion between, for example, a negative region on both the acid and base, or if both were positive.

The work described below consists of an exhaustive test of this hypothesis. By appropriate manipulation of substituents, a number of bases are designed whose MEP is positive in the vicinity of their lone pair, or in other cases around their π-electron densities, as opposed to the usual negative potential. The possibility that they might nonetheless engage in a XB with a positively charged σ-hole on a partner Lewis acid is assessed via quantum chemical calculations. In the same vein, several acids wherein the σ-hole on the halogen atom bears a negative MEP are combined with a Lewis base to determine whether a XB is possible between them.

METHODS

Quantum chemical calculations were performed via the Gaussian 16 [30] set of codes, applying density functional theory (DFT) in the framework of the M06-2X functional [31], along with the polarized def2-tzvp basis set. The latter contains an effective core potential for fourth-row I and Te which takes partial account of relativistic effects. There is ample confirmation in the literature of the reliability of this approach [32-38]. The interaction energy E_{int} of each dyad was calculated as the difference between the energy of the complex and the sum of the energies of the Lewis acid and base, each in the context of the geometry they adopt within the dimer. Basis set superposition error was corrected by the counterpoise procedure [39]. The Multiwfn program [40] evaluated the molecular electrostatic potential (MEP) and located and quantified the extrema residing on the ρ=0.001 au isodensity surface of each optimized monomer. Bond paths were located by the QTAIM formalism, and the density at the bond critical point evaluated by AIMAll software [41]. Charge transfers between individual orbitals and their associated second-order energies, were derived by Natural Bond Orbital (NBO) theory [42, 43] by way of the NBO program incorporated within Gaussian. The interaction energies of the dimers were partitioned into physically meaningful components via the SAPT0 prescription [44-47] within the Psi4 program [48].

RESULTS

The results are divided as follows. The source of electrons from the first set of bases considered are the π-systems of alkynes, alkenes, and a phenyl ring. Replacement of their H atoms by the electron-withdrawing F draw density away from the π-system, leaving it with a reduced negative, or even positive potential. The second section extends this notion of a positive

π-region to heteroatomic C=Y bonds where Y represents one of several chalcogen atoms O, S, or Te. The possibility of designing a ZR_3 base where the lone pair of the central pnicogen atom, N or P, sits in a region of positive potential is the subject of the next section. Each of these various bases are paired with a IC≡CH Lewis acid which contains a fairly deep positive σ-hole on the I atom so as to maximize the possibility of formation of a halogen bond. The final section reverses the pattern and considers whether a Lewis acid which has a negatively charged σ-hole can nonetheless engage in a X··N halogen bond. The NH_3 molecule is taken as the universal base in this series of calculations, given its high basicity and the availability of its lone pair. ICCH and NH3 have the additional advantage of their small size, making it unlikely they will engage in secondary interactions other than the XB that would complicate the analysis.

C=C π-bonds

The red areas of Fig 1a-c show the negative potentials that lie above the C-C midpoints of the unsubstituted unsaturated C_2H_2, C_2H_4, and C_2H_6 systems, coinciding with their π-systems. (It might be noted that the region directly above the center of benzene is not quite as negative as directly above the C atoms; see below.) One way of characterizing the magnitudes of these negative regions rests on the prescription of locating the minimum of the MEP on an isodensity surface, typically ρ=0.001 au, commonly referred to as $V_{min,S}$. The first three rows of Table 1 show that these unsubstituted systems all present a fairly strong negative MEP; both acetylene and ethylene have a $V_{min,S}$ of -16 kcal/mol. The area lying over the center of the benzene ring is equally negative, with $V_{min,S}$ equal to -17 kcal/mol.

In order to circumvent the arbitrariness of this particular prescription, the MEP was evaluated along a line emanating from the center of the relevant C=C or C≡C bond, or from the center of the ring in the case of benzene. This line was oriented perpendicular to the bond, corresponding to the π region over the molecule. The three lower curves in Fig 2 show how each MEP is negative even for long distances d from the bond center, becoming more so as the reference point moves in, until finally beginning to curve upwards at distances less than about 1.6-1.8 Å from the midpoint. One can take the minimum of each curve in Fig 2 as an alternate measure of the most negative MEP, referred to here as $V_{min,Ax}$. Comparison of the second with the first column of Table 1 indicates $V_{min,Ax}$ along this axis is quite similar to that on the isodensity surface, $V_{min,S}$.

Given the negative potential in this π-region, it is not surprising that each of these three systems engages in a moderately strong XB with ICCH, between 3 and 4 kcal/mol, listed in Table 1 as E_{int}. The geometry of these complexes shown in Fig 1g-i places ICCH perpendicular to the C=C or C≡C bond, with I equidistant from the two C atoms. These R(I··mid) distances are 3.32 for the alkene and alkyne. In part due to the aforementioned lower MEP over the C atoms than over the benzene center, the I atom of ICCH is displaced a bit toward one of the six C-C pairs, with R=3.46 Å, slightly longer than this distance in the acetylene or ethylene systems. In all cases, NBO reveals a substantial charge transfer from the π(CC) bond to the σ*(CI) antibonding orbital of ICCH, listed in the penultimate column of Table 1.

Perfluorosubstitution of each of these hydrocarbons will draw density away from the C atoms and their π-bonds, which ought to make V_{min} less negative or even positive. This effect is obvious in a comparison of the fluorinated molecules in Fig 1d-f with their unsubstituted counterparts immediately above. As can be seen in Table 1, C_2F_2 takes on a $V_{min,S}$ that is barely negative, while the other two molecules have fairly substantial positive values. The rise in MEP is also evident along the axis perpendicular to the π-bond by the shapes of the three upper curves in Fig 2. The C_2F_2 MEP contains a minimum of -2.1 kcal/mol at about d=1.8 Å, but the other two fluorinated units show a steady rise as d diminishes, and hence no $V_{min,Ax}$.

Given the overall positive potential in the π-region it is perhaps counterintuitive that all three of these fluorinated units can engage in a XB with ICCH. The interaction energies are between 1 and 2 kcal/mol, somewhat weaker than the unsubstituted parallels. And the intermolecular distances are a bit longer, but only slightly. Each of these interactions can be fairly characterized as a true XB, with an AIM bond path that extends from the I to the C-C midpoint of the alkene and alkyne with a bcp density of 0.01. The bond path involving the phenyl ring terminates on one of the C atoms, the one which is closest to I. The density of this BCP is slightly smaller, 0.008. All systems are characterized by a substantial NBO π(CC)→σ*(CI) E2, varying from 1 kcal/mol for the phenyl rings, and as high as 3 kcal/mol for the alkene and alkyne. As another marker, the last column of Table 1 displays the total natural charge of all the atoms of each subunit within the complex, so verifies that there is indeed a net transfer of charge from the π-system to the ICCH Lewis acid, as would be expected for a XB. This quantity lies in the range of 10-17 me.

Given the variability of both the magnitude and even the sign of the MEP in the region of the π-density, it is natural to wonder how the electrostatic portion of the interaction varies for each complex. The fourth column of data in Table 1 lists the electrostatic component (ES) of a SAPT decomposition of each of these XBs. Not unexpectedly, ES is substantial and negative (attractive) for all of the unsubstituted Lewis bases. It remains negative, albeit smaller in magnitude, for C_2F_2, consistent with the small magnitude of its V_{min}. More surprising is that ES remains negative (attractive) for both C_2F_4 and C_6F_6, despite the fairly large positive $V_{min,S}$, and the complete absence of a $V_{min,Ax}$ for these two bases.

There are two principal factors that help explain this apparent contradiction. In the first place, the ES component results from Coulombic contacts between the entireties of both molecules, not just the oversimplified view of a single pointwise contact between V_{min} of one molecule with V_{max} of the other. Secondly, as the two molecules approach one another, there is a certain degree of mutual penetration of the two charge clouds, which can add to the attractive quality of this term [49]. It is perhaps due to these issues that ES for the interaction of HCCI with C_6F_6 is slightly more negative than that for C_2F_4 even though the former has a more positive V_{min}.

Table 2 lists all of the various components of the SAPT decomposition of the interaction energy of each halogen-bonded complex. One can see that the perfluorosubstitution yields a slight reduction in both the induction (IND) and the dispersion (DISP) energies, but that these

changes are dwarfed by the reductions in ES. The last column of Table 2 displays the percentage contribution made by ES to the cumulative attractive portion (ES+IND+DISP). While ES accounts for between 1/3 and 1/2 of this total for the unsubstituted systems, this percentage shrinks down below 35% for the fluorinated bases, and barely more than 10% for the last two. So in conclusion, the change in overall sign of the MEP above these π-systems from negative to positive reduces, but does not eliminate, the ability of these bases to form a XB with ICCH, nor does it eliminate the attractive nature of the electrostatic component of the interaction energy.

Heteronuclear π-bonds

π-bonds are of course not limited to pairs of identical C atoms. Molecules related to formaldehyde are also of interest, in which a C engages in a double bond with a chalcogen atom. Four such molecules were considered here. As a point of reference, the two F atoms of F_2CO ought to draw a good deal of density from the C=O bond, leaving the region above the plane with a positive potential, despite the density which would be available to share with an approaching electrophile. Replacing the atoms surrounding the central C by less electron-withdrawing ones, as in H_2CS ought to allow the potential above the plane to become less negative, perhaps even positive. Further replacement of the two H atoms by electron-donating methyl groups should amplify this effect. Changing the S to the larger and less electronegative Te atom in Me_2CTe would exaggerate the difference between C and its bonding chalcogen neighbor.

Fig 3a-d shows that the region lying above these C=Y atoms, where Y represents any of the chalcogen atoms, does not appear to take on a negative MEP, which is concentrated instead in the molecular plane. Indeed, a scan of the vdW surface, characterized by ρ=0.001 au, does not provide a $V_{min,S}$ for any of these molecules, as indicated by the x markings in the first column of Table 3. Indeed, all minima on this particular surface lie within the plane of the molecule. So from that perspective, none of these molecules are prone to donate density in a XB.

A view of the MEP along an axis perpendicular to the molecule offers a somewhat different interpretation, however. The curves in Fig 4 are measured along a line that stretches upward from the midpoint of each C=Y bond axis, perpendicular to the molecule. The upper purple curve documents the overwhelming positive nature of the MEP of the π-region of F_2CO which only becomes more positive as the point of reference approaches the molecular plane. The other curves are quite different in character, showing that the MEP is negative along this axis, and becomes more so until a minimum is reached for distances less than 2.5 Å. As reported in Table 3, the MEP is equal to -2 kcal/mol for this $V_{min,Ax}$ of H_2CS, and reaches down further to -6 kcal/mol for both Me_2CS and Me_2CTe.

While neither F_2CO with its positive MEP, nor H_2CS with its very shallow $V_{min,Ax}$ are capable of sustaining a XB, the latter two molecules with their more negative minimum do so. These bonds are fairly strong, with interaction energies of about 4 kcal/mol, as listed in Table 3. The I atom approaches to within about 3.4-3.5 Å of the C=Y midpoint, only slightly longer than in the homonuclear C-C bonds in Table 1. Because of the more negative potential above the Y

than over the C, Fig 3e and 3f show that the HCCI molecule points almost directly to the Y atom. The AIM bond path is curious. In the case of Me_2CS, the path veers toward the S atom in Fig 3g, while it takes a sudden turn toward C for Me_2CTe in Fig 3h. Nonetheless, the bond critical point densities are both 0.01 au, and there is a sizable E2 of around 3 kcal/mol. The substantially negative ES components of roughly -5 kcal/mol for the two methylated bases in Table 3 are consistent with the negative MEP above the molecular plane. All of the SAPT components contained in Table S1 complete this picture with a strongly attractive DISP, and a smaller induction energy.

Lone Pairs

Even more than π-bonding regions, the most common source of electron density donation within a XB is the lone pair of a Lewis base. The MEP is typically rather negative in the region of a lone pair, as in the prototypical case of NH_3 which has a $V_{min,S}$ of -40.1 kcal/mol, as listed in the first row of Table 4. This molecule easily forms a rather strong XB with ICCH of 6.6 kcal/mol. The BCP density is 0.019 au, and there is a large E2 of 8.3 kcal/mol for transfer from the N lone pair to the σ*(CI) orbital. Changing the N hybridization from sp^3 to sp, as in NCF and $NCNO_2$, reduces the negative value of $V_{min,S}$ and consequently the XB strength along with its various markers.

But one can imagine scenarios that might make the MEP less negative or even positive in the region of the lone pair. Replacing the three H atoms of NH_3 by F reduces $V_{min,S}$ down to only -3.9 kcal/mol. This transformation is more vividly shown in the comparison of the MEPs of these two molecules in Fig 5a and 5b. Table 4 further shows that use of three NO_2 substituents reverses the sign of $V_{min,S}$, as does changing the N of NF_3 to the less electronegative P, with their MEPs in Fig 5 consistent with this pattern. The radial dependence of the MEP of each molecule along its lone pair C_3 rotation axis in Fig 6 (or CN axis for NCF and $NCNO_2$) fits these observations. The MEP of $N(NO_2)_3$ and PF_3 are positive for any distance from the central atom just as NH_3, NCF, $NCNO_2$, and NF_3 are negative. Each molecule does contain a shallow minimum in its axial MEP, whose characteristics are contained in Table 4, but the value of this $V_{min,Ax}$ differs little from $V_{min,S}$.

The four former systems with the negative V_{min} form stable XBs with ICCH, as might be expected, and with their interaction energies varying in line with the MEP minima. More surprising though is the ability of both $N(NO_2)_3$ and PF_3 to also participate in such a bond, despite their positive MEP minimum. In fact, these two XBs are slightly stronger than that involving NF_3 with its negative V_{min}. The geometry of each such system points the I directly toward the central Z, with the AIM bond path connecting them. All six of these XBs are confirmed as such by their substantial bond critical point densities and E2 for $Z_{lp}\rightarrow\sigma^*(CI)$ transfer where Z represents either N or P. Further verification arises in connection with the net charge transferred from the Lewis base to the ICCH acid. The intermolecular distances are all substantially shorter than the sum of vdW distances of 3.70 Å for I··N and 3.94 Å for I··P [50].

Even for the two XBs with positive V_{min}, and with interaction energy barely above 1 kcal/mol, the ratio of the XB distance to the vdW sum is 0.9.

It is understandable that ES declines along with V_{min}. However, one sees again that a positive MEP does not preclude either a stable XB or an attractive ES component, as may be seen for both $N(NO_2)_3$ and PF_3. The complete SAPT decomposition of these complexes in Table S2, shows that the percentage ES contribution declines along with the diminishing V_{min}, from a maximum of 61% for NH_3, down to only 15% for $N(NO_2)_3$. The ES term for PF_3 is disproportionately large for its small V_{min}, perhaps due to an elevated degree of charge penetration within the complex.

σ-Holes

As a converse to the issue concerning electron donors with positive MEP, there is the question as to whether a Lewis acid can engage in a XB if its σ-hole region is negative. Although there might be some electrostatic repulsion with an incoming nucleophile, there remains the stabilizing influence of charge transfer into the σ* antibonding orbital of the acid. So as to answer this question, a series of Lewis acids were constructed that contained σ-holes with negative as well as positive MEP. Each was then allowed to interact with NH_3 as a prototype base with a prominent lone pair.

The Lewis acid candidates are listed in Table 5, along with the value of the MEP on their ρ=0.001 au isodensity surface as $V_{max,S}$. The low electronegativity of Ge reduces the pull on the electron density of the Ge-X covalent bond. But even so, GeH_3I has a positively charged σ-hole with $V_{max,S}$=+7.6 kcal/mol. However, replacing I by its smaller and more electronegative Br counterpart brings this quantity down to slightly below zero, while the σ-hole on GeH_3Cl reaches down to -7.1 kcal/mol. The electron-releasing capability of the methyl group imbues both $GeMe_3Br$ and $GeMe_3I$ with a negative $V_{max,S}$, particularly the former with a minimum of -8.8 kcal/mol. As an alternative molecular structure, the halogen atom was placed on a permethylated phenyl ring. However, as may be seen in the last two rows of Table 5, although the σ-hole MEP is rather small, it remains positive for both C_6Me_5Br and C_6Me_5Cl.

The radial behavior of the MEP was examined by plotting it along a line emanating from the X atom, as an extension of each T-X covalent bond. The behavior of the MEP along this axis, illustrated in Fig 7, is interesting from a number of perspectives. In the first place, whether the MEP is positive or negative at the specific distance d which corresponds to ρ=0.001 au, it is negative at long range. For example, the MEP of even GeH_3I, which has a $V_{max,S}$ value of +7.6 kcal/mol, sinks below 0 for d > 2.8 Å. Each of the curves in Fig 7 becomes progressively more positive as the reference point more closely approaches the X atom, although several do display a shallow minimum. GeH_3Cl, for example, has its most negative MEP of -8.2 kcal/mol for d=2.4 Å, which is marginally more negative than its value of -7.1 kcal/mol on the ρ=0.001 au isodensity surface for which d=2.02 Å. Importantly, in no case does the presence of such a shallow minimum on the radial function in Fig 7 reverse the conclusion from the isodensity surface of the sign of V_{max}.

Perusal of Table 5 shows that it is difficult to form a XB if the σ-hole has a negative charge, although it is not necessary for $V_{max,S}$ to be highly positive. More specifically, GeH_3I with its substantial MEP maximum of 7.6 kcal/mol forms a I··N XB with NH_3 with E_{int}=1.63 kcal/mol, and C_6Me_5Br is right behind, with values of +4.6 and 1.25 kcal/mol, respectively. The structures of these two complexes are illustrated in Fig 8a and 8c, respectively. Reducing $V_{max,S}$ to only +0.4 kcal/mol still allows C_6Me_5Cl to form a XB, even if quite weak at 0.45 kcal/mol (Fig 8d). The further slight reduction of $V_{max,S}$ to the negative value of -0.4 kcal/mol retains this ability for GeH_3Br in Fig 8b. The other quantities listed in Table 5 confirm these interactions to be true XBs, with ρ_{BCP}~0.01 au and with E2 between 1.3 and 3.1 kcal/mol, along with an overall charge transfer of 3-11 me. The R/R_{vdW} ratio is equal to 0.90 for three of these complexes, with the exception being the weak XB with GeH_3Br, with its slightly negative V_{max}, for which this ratio is 0.96. In accord with the positive values of V_{max}, the ES component listed in Table 5 is negative, even for GeH_3Br, whose MEP maximum is slightly negative. The percentage contribution of ES to each of these XBs lies between 35% and 51%, as reported in Table S3, where the higher percentages correlate with the deeper σ-holes. On the other hand, the other three systems with more negative σ-holes, even only slightly negative at -1.9 kcal/mol as in the case of $GeMe_3I$, remove this possibility.

DISCUSSION

It would appear then that a negatively charged minimum of the MEP of the base, in the vicinity of the electrons that will be partially transferred to the Lewis acid, is certainly beneficial for formation of a XB but is not necessary in all cases. The perfluorinated ethylene and benzene molecules are examples in that both form a XB with the ICCH unit, but the MEP lying above their π-clouds is positive. This positive charge is not confined only to the vdW surface, but extends over the entire range of a line emanating from the center of the molecule. This idea is also carried over to the lone pair of the N and P atoms. Both $N(NO_2)_3$ and PF_3 form a XB, despite a positively charged MEP along the C_3 axis that includes the lone pair that donates charge to the acid unit.

In the case of a Lewis acid, a positively charged σ-hole, coincident with the antibonding σ*(TX) orbital, clearly represents an optimal situation for engagement with a Lewis base. However, the question of the sign of the MEP is a bit more nuanced. It would appear that the MEP along the extension of the T-X bond is always negative at long range, regardless of the nature of the Lewis acid. The MEP becomes less negative as the reference point approaches more closely, eventually turning positive at some particular distance, which differs for each acid. So the question as to whether the σ-hole region is positive or negative depends upon the distance chosen for its evaluation. This transition point from negative to positive is equal to 2.9 Å for GeH_3I, for example, but is much smaller at 1.7 Å for GeH_3Cl. In the former case, the transition distance is much longer than the vdW radius of I (2.04 Å), while the 1.7 Å transition distance of GeH_3Cl is somewhat shorter than the Cl vdW radius of 1.82 Å. It is for this reason that one can speak of a positively charged σ-hole for the former while the latter's MEP can be considered

negative, adopting the stance that it is the magnitude of the MEP at the vdW surface which is the decisive factor.

From this standpoint, it would appear that the σ-hole region must be characterized by a positive MEP on its vdW surface, even if only by a small amount, in order to sustain a XB. The only exception to this rule is GeH_3Br, for which $V_{max,S}$ is only barely negative at -0.4 kcal/mol. The interaction energy involved in its XB with NH_3 is very small, only 0.4 kcal/mol.

On the other hand, one might expect that pairing up with a stronger base might strengthen some of these weak XBs, or even permit the formation of such a bond with an acid with a negative V_{max}. To examine this issue, some of the acids with questionable σ-holes were paired with NMe_3, whose three electron-donating methyl substituents amplify the availability of its lone pair. This switch of bases raises the interaction energy of GeH_3Br, whose $V_{max,S}$ is slightly negative, from 0.44 to 1.51 kcal/mol. $GeMe_3I$, which was incapable of engaging in a XB with NH_3, has an even more negative $V_{max,S}$ of -1.9 kcal/mol. Amping up the base strength with NMe_3 promotes its formation of a XB, with interaction energy 1.78 kcal/mol, despite the negative $V_{max,S}$.

The MEP of the σ-hole of GeH_3Cl is more substantially negative, -7.1 kcal/mol. Adding NMe_3 as a partner permits a certain level of engagement, but the base is twisted so that its lone pair is not oriented correctly toward Cl, displaced by 35°. AIM bond paths lead from Cl not only to the N, but also to two methyl H atoms, so this complex is held together by two CH··Cl HBs, as well as any weak Cl··N XB. With a cumulative E_{int} of -0.86 kcal/mol, it would be difficult to ascribe a substantive XB to this complex.

Invoking charge assistance by placing a negative charge on the base can be an important amplification factor [51-59]. When the base was mutated to Cl^-, this anion situated itself directly along the Ge-Cl axis of GeH_3Cl with R(Cl···Cl)= 3.223 Å, but with only a slightly negative interaction energy of -0.34 kcal/mol. AIM and NBO analysis point to a XB as the sole source of stability of this dimer.

Just as the depth of a σ-hole is a nettlesome question, requiring some consideration as to the distance from the X atom, so too is there a certain degree of uncertainty in assessing the potential associated with a source of electron density. For systems like C_6F_6 and C_2F_4, the potential is clearly positive above the molecular plane, but the value of the MEP is quite sensitive to the distance of the reference point. As another situation, the MEP above the C≡C bond of C_2F_2 undergoes a change of sign, from positive to negative, and then back to positive for closer approach. Even for the unsubstituted unsaturated systems for which the MEP is negative definite, there is a particular distance for which this MEP is at its minimum, which does not necessarily coincide with the vdW distance. Some of these ideas extend beyond the π-systems, and are common to the lone pair of the nucleophile. Whether the MEP is positive or negative along the lone pair axis, it bottoms out at a particular distance, before rising quickly as the reference point more closely approaches the atom in question.

Given the minor contribution of the ES component to the interaction energy of some of these complexes, particularly those with small negative or even positive V_{min} on the base, it is natural

to wonder if the XB strength would deteriorate or strengthen if the σ-hole of the Lewis acid is weakened. In comparison to $V_{max,S}$ of 34.8 kcal/mol for ICCF, binding the I to a sp^3 methyl group in CH_3I reduces this quantity to 13.7 kcal/mol. Switching out the I for a Cl leads to a slightly negative $V_{max,S}$ of -1.3 for CH_3Cl. The interaction energies of these two acids with C_2F_4 ($V_{min,S}$ = +10.7 kcal/mol) were computed to be 1.25 and 1.19 kcal/mol, respectively, hardly changed from the 0.95 kcal/mol arising from ICCH, despite a 36 kcal/mol range of σ-hole depths for the three acids. In a similar vein related to a lone pair rather than a π-region, the interaction energies of CH_3I and CH_3Cl with $N(NO_2)_3$ ($V_{min,S}$ = +4.0 kcal/mol) are respectively 1.39 and 1.24 kcal/mol, again barely changed from the value of 1.33 kcal/mol for ICCH. This nearly uniform quantity implies that the binding energy of a Lewis acid to a base with a small or positive MEP is largely independent of the identity of the acid, or the depth of its σ-hole.

A deeper insight into this behavior can be gleaned by an energy decomposition of each of these very similar total interaction energies, and a comparison with bases that have a true negative MEP. As is evident in Table 6, The ES components involving unsubstituted NH_3 are quite negative, making up well over half of the total attractive energy. The magnitude of ES is cut in half as the acid changes from ICCH to ICH_3, in concert with the much shallower σ-hole of the latter. (In fact, the slightly negative V_{max} of $ClCH_3$ prevents it from forming a Cl··N XB with NH_3 at all.) Note also the dropping IND and DISP components that accompany the weakening bond. When combined with EX, the total SAPT interaction energy drops markedly as the σ-hole is weakened, vanishing entirely for $ClCH_3$. The contrast is obvious for $N(NO_2)_3$ with its positive MEP in the N lone pair region. In the first place, the total SAPT energy is rather static at around 2 kcal/mol, in fact rising a bit as the σ-hole on the acid weakens. This strengthening bond can be attributed to the ES term which, although small in magnitude, rises as the acid V_{max} drops, thereby reducing Coulombic repulsion with the N lone pair's positive MEP.

Very similar trends are apparent for the X··π bonds in the lower half of Table 6. Again, the ES component is sizable for the unsubstituted alkene with its negative π MEP, making up nearly half of the total. The shallower σ-hole of ICH_3 cuts ES, as well as the other components, resulting in a weaker overall XB. When the four F substituents are added to the alkene, making its π-region positive, one again sees a much smaller ES, which rises in magnitude as the acid V_{max} drops. Indeed, ES triples in the mutation of the acid from ICCH to $ClCH_3$. Even so, the percentage contribution of ES remains under 40%. As in the lone pair cases, the total SAPT energy is fairly insensitive to the particular acid as the increasing ES is opposed by reduced IND and DISP, also resulting in a larger proportional contribution of ES to the total.

There have been some earlier indications that the approach of regions of like-charged MEPs of two neutral molecules might not be fully repulsive. For example, Ibrahim and coworkers showed that small negative interaction energies can be calculated when two molecules were oriented so that their positively charged σ or π-holes approached one another [60, 61]. However, it is unclear if these geometries represented true minima as the orientations were rigidly enforced. SAPT partitioning offered small negative electrostatic components, consistent with the finding present above. There is also some computational evidence that the positive MEP situated above

C_6F_6 can interact with the positive π-hole of a partner molecule [62], again with a small negative ES component, although again the enforcement of geometric restrictions did not permit the identification of these complexes as true minima.

Zhang and Wang [63] discussed a configuration where two positively charged σ-holes might interact attractively with one another in the context of several intriguing crystal structures. These interactions were assessed to be dispersion-dominated, with minor but attractive ES components, not unlike the SAPT findings here. Likewise, other calculations found instances of attractive forces between a σ-hole and π-hole, both positively charged [64], with total interaction energies in the 1 kcal/mol range. Wang et al [65] had argued that electrostatic repulsion between electrophilic sites can be overcome by charge transfer and dispersion, and provided examples of stable interactions between positively charged σ-holes.

Another recent work [66] found that a positively charged region located above the S or Se atom of planar 2,3,4,5-tetrafluorothiophene or -selenophene (termed a π-lump) could engage in a XB with the σ-hole of dihalogen molecules. The two rings contained fairly small $V_{max,S}$ values of 3.4 and 2.8 kcal/mol, respectively, helping to minimize Coulombic repulsions. Despite this point-to-point repulsion, the authors found fairly large negative electrostatic components, which they attributed to charge penetration.

In the same context of chalcogen atoms, recent calculations [25] showed that even a negative $V_{max,S}$ of a σ-hole on a chalcogen (Ch=S or Se) atom within a XYT=Ch molecule where T represents a tetrel atom appear capable of forming a ChB with a N-base, albeit exceedingly weak ones, less than 1 kcal/mol. Unlike the systems examined here, the electrostatic components of these chalcogen bonds are repulsive. This work pointed out also that these negative σ-holes reverse their sign as the reference point comes closer to the S or Se atom, more representative of the position of the base atom.

The idea that a positive region near a lone pair or π-system of a base might interact with the positive σ-hole of an approaching Lewis acid might be thought of as anti-electrostatic, although that particular term has usually been employed in the discussion of fully charged ions, as in cation-cation or anion-anion [67, 68]. Pairs of this sort are typically unstable unless they are immersed in a simulated solvent of some sort, or a series of counterions have been added, to disperse the charges and minimize Coulombic repulsions [69-78]. In some cases, metastable complexes can be identified in the gas phase, but these are higher in energy than the separated monomers [25, 79-85]. Fully stable minima can be achieved in the gas phase if the two cations are large enough that there is large separation between their centers of like charge [86, 87].

CONCLUSIONS

The generic halogen bond strengthens as the negative potential of the base rises in magnitude. However, a XB can be formed even if this potential becomes positive. C_2F_4 and C_6F_6 are cases in point, where the minimum in the potential above the π-systems of these nucleophiles is as high as +16 kcal/mol. Placing strongly electron-withdrawing substituents on a N or P atom can leave its lone pair region with an overall positive potential, which is still capable

of forming a XB. Although these interactions carry all of the markers of true XBs, with appropriate charge transfers and AIM bond paths, they are fairly weak, less than 2 kcal/mol. In the converse situation it does appear that a positively charged σ-hole is required for a Lewis acid to engage in a XB in most cases, as even a slightly negative potential discourages such a bond, although a weak XB can be coaxed with a particularly strong base. It is particularly intriguing that, unlike mainstream halogen bonds, these systems with either positive potentials near the electron source of the base, or a negative σ-hole region on the acid, cannot be significantly strengthened by changing the characteristics of the partner molecule.

Funding

This research was funded by the US National Science Foundation under Grant No. 1954310.

Conflicts of Interest

The author declares no conflict of interest.

REFERENCES

1. S. N. Vinogradov and R. H. Linnell, *Hydrogen Bonding*, Van Nostrand-Reinhold, New York, 1971.
2. M. D. Joesten and L. J. Schaad, *Hydrogen Bonding*, Marcel Dekker, New York, 1974.
3. P. Schuster, G. Zundel and C. Sandorfy, *The Hydrogen Bond. Recent Developments in Theory and Experiments*, North-Holland Publishing Co., Amsterdam, 1976.
4. M. M. Szczesniak, S. Scheiner and Y. Bouteiller, *J. Chem. Phys.*, 1984, **81**, 5024-5030.
5. S. Cybulski and S. Scheiner, *J. Am. Chem. Soc.*, 1987, **109**, 4199-4206.
6. G. Gilli and P. Gilli, *The Nature of the Hydrogen Bond*, Oxford University Press, Oxford, UK, 2009.
7. S. Horowitz, L. M. A. Dirk, J. D. Yesselman, J. S. Nimtz, U. Adhikari, R. A. Mehl, S. Scheiner, R. L. Houtz, H. M. Al-Hashimi and R. C. Trievel, *J. Am. Chem. Soc.*, 2013, **135**, 15536-15548.
8. I. Alkorta and A. C. Legon, *ChemPlusChem*, 2021, **86**, 778-784.
9. J. E. Del Bene, I. Alkorta and J. Elguero, *Chem. Phys. Lett.*, 2020, **761**, 137916.
10. D. F. Mertsalov, R. M. Gomila, V. P. Zaytsev, M. S. Grigoriev, E. V. Nikitina, F. I. Zubkov and A. Frontera, *Cryst.*, 2021, **11**, 1406.
11. S. V. Baykov, D. M. Ivanov, S. O. Kasatkina, B. Galmés, A. Frontera, G. Resnati and V. Y. Kukushkin, *Chem. Eur. J.*, 2022, **28**, e202201869.
12. R. D. Parra and S. J. Grabowski, *Int. J. Mol. Sci.*, 2022, **23**, 11289.
13. P. Politzer, P. Lane, M. C. Concha, Y. Ma and J. S. Murray, *J. Mol. Model.*, 2007, **13**, 305-311.
14. M. Michalczyk, W. Zierkiewicz and S. Scheiner, *Cryst. Growth Des.*, 2022, **22**, 6521-6530.
15. C. I. Yeo, Y. S. Tan, H. C. Kwong, V. S. Lee and E. R. T. Tiekink, *CrystEngComm*, 2022, **24**, 7579-7591.

16. S. Scheiner, *J. Phys. Chem. A*, 2022, **126**, 6443-6455.
17. M. Michalczyk, B. Kizior, W. Zierkiewicz and S. Scheiner, *Phys. Chem. Chem. Phys.*, 2023, **25**, 2907-2915.
18. S. Scheiner, *Phys. Chem. Chem. Phys.*, 2021, **23**, 5702-5717.
19. E. Alikhani, F. Fuster, B. Madebene and S. J. Grabowski, *Phys. Chem. Chem. Phys.*, 2014, **16**, 2430-2442.
20. H. S. Biswal, A. K. Sahu, B. Galmés, A. Frontera and D. Chopra, *ChemBioChem*, 2022, **23**, e202100498.
21. B. Galmés, A. Juan-Bals, A. Frontera and G. Resnati, *Chem. Eur. J.*, 2020, **26**, 4599-4606.
22. W. Zierkiewicz, M. Michalczyk, G. Mahmoudi, I. García-Santos, A. Castiñeiras, E. Zangrando and S. Scheiner, *ChemPhysChem.*, 2022, **23**, e202200306.
23. P. R. Varadwaj, A. Varadwaj, H. M. Marques and K. Yamashita, *Int. J. Mol. Sci.*, 2022, **23**, 1263.
24. K. T. Mahmudov, A. V. Gurbanov, V. A. Aliyeva, M. F. C. Guedes da Silva, G. Resnati and A. J. L. Pombeiro, *Coord. Chem. Rev.*, 2022, **464**, 214556.
25. R. Wysokiński, W. Zierkiewicz, M. Michalczyk and S. Scheiner, *Molecules*, 2021, **26**, 6394.
26. J. E. Del Bene, I. Alkorta and J. Elguero, *Mol. Phys.*, 2019, **117**, 1117-1127.
27. I. Alkorta and A. Legon, *Molecules*, 2018, **23**, 2250.
28. S. J. Grabowski, *Phys. Chem. Chem. Phys.*, 2014, **16**, 1824-1834.
29. S. Scheiner, *J. Phys. Chem. A*, 2021, **125**, 2631-2641.
30. M. J. Frisch, G. W. Trucks, H. B. Schlegel, G. E. Scuseria, M. A. Robb, J. R. Cheeseman, G. Scalmani, V. Barone, G. A. Petersson, H. Nakatsuji, X. Li, M. Caricato, A. V. Marenich, J. Bloino, B. G. Janesko, R. Gomperts, B. Mennucci, H. P. Hratchian, J. V. Ortiz, A. F. Izmaylov, J. L. Sonnenberg, Williams, F. Ding, F. Lipparini, F. Egidi, J. Goings, B. Peng, A. Petrone, T. Henderson, D. Ranasinghe, V. G. Zakrzewski, J. Gao, N. Rega, G. Zheng, W. Liang, M. Hada, M. Ehara, K. Toyota, R. Fukuda, J. Hasegawa, M. Ishida, T. Nakajima, Y. Honda, O. Kitao, H. Nakai, T. Vreven, K. Throssell, J. A. Montgomery Jr., J. E. Peralta, F. Ogliaro, M. J. Bearpark, J. J. Heyd, E. N. Brothers, K. N. Kudin, V. N. Staroverov, T. A. Keith, R. Kobayashi, J. Normand, K. Raghavachari, A. P. Rendell, J. C. Burant, S. S. Iyengar, J. Tomasi, M. Cossi, J. M. Millam, M. Klene, C. Adamo, R. Cammi, J. W. Ochterski, R. L. Martin, K. Morokuma, O. Farkas, J. B. Foresman and D. J. Fox, Wallingford, CT2016.
31. Y. Zhao and D. G. Truhlar, *Theor. Chem. Acc.*, 2008, **120**, 215-241.
32. K. Kříž and J. Řezáč, *Phys. Chem. Chem. Phys.*, 2022, **24**, 14794-14804.
33. D. Wu and D. G. Truhlar, *J. Chem. Theory Comput.*, 2021, **17**, 3967-3973.
34. A. D. Boese, *ChemPhysChem.*, 2015, **16**, 978-985.
35. A. Li, H. S. Muddana and M. K. Gilson, *J. Chem. Theory Comput.*, 2014, **10**, 1563-1575.
36. S. Kozuch and J. M. L. Martin, *J. Chem. Theory Comput.*, 2013, **9**, 1918-1931.
37. M. Walker, A. J. A. Harvey, A. Sen and C. E. H. Dessent, *J. Phys. Chem. A*, 2013, **117**, 12590-12600.
38. N. Mardirossian and M. Head-Gordon, *J. Chem. Theory Comput.*, 2013, **9**, 4453–4461.
39. S. F. Boys and F. Bernardi, *Mol. Phys.*, 1970, **19**, 553-566.
40. T. Lu and F. Chen, *J. Comput. Chem.*, 2012, **33**, 580-592.
41. T. A. Keith, TK Gristmill Software, Overland Park KS2013.

42. A. E. Reed, L. A. Curtiss and F. Weinhold, *J. Chem. Phys.*, 1985, **83**, 735-746.
43. A. E. Reed, L. A. Curtiss and F. Weinhold, *Chem. Rev.*, 1988, **88**, 899-926.
44. K. Szalewicz and B. Jeziorski, in *Molecular Interactions. From Van der Waals to Strongly Bound Complexes*, ed. S. Scheiner, Wiley, New York1997, pp. 3-43.
45. R. Moszynski, P. E. S. Wormer, B. Jeziorski and A. van der Avoird, *J. Chem. Phys.*, 1995, **103**, 8058-8074.
46. K. E. Riley and P. Hobza, *J. Chem. Theory Comput.*, 2008, **4**, 232-242.
47. K. Szalewicz and B. Jeziorski, *J. Mol. Model.*, 2022, **28**, 273.
48. D. G. A. Smith, L. A. Burns, A. C. Simmonett, R. M. Parrish, M. C. Schieber, R. Galvelis, P. Kraus, H. Kruse, R. D. Remigio, A. Alenaizan, A. M. James, S. Lehtola, J. P. Misiewicz, M. Scheurer, R. A. Shaw, J. B. Schriber, Y. Xie, Z. L. Glick, D. A. Sirianni, J. S. O'Brien, J. M. Waldrop, A. Kumar, E. G. Hohenstein, B. P. Pritchard, B. R. Brooks, H. F. SchaeferIII, A. Y. Sokolov, K. Patkowski, A. E. DePrinceIII, U. Bozkaya, R. A. King, F. A. Evangelista, J. M. Turney, T. D. Crawford and C. D. Sherrill, *J. Chem. Phys.*, 2020, **152**, 184108.
49. E. M. Cabaleiro-Lago, J. Rodríguez-Otero and S. A. Vázquez, *Phys. Chem. Chem. Phys.*, 2022, **24**, 8979-8991.
50. S. Alvarez, *Dalton Trans.*, 2013, **42**, 8617-8636.
51. S. J. Grabowski, *Cryst. Growth Des.*, 2023, **23**, 489-500.
52. C. A. Montgomery, I. Jameel, F. Cuzzucoli, T. Chidley, W. S. Hopkins and G. K. Murphy, *Chem. Eur. J.*, 2022, **28**, e202202029.
53. A. N. Usoltsev, N. A. Korobeynikov, B. A. Kolesov, A. S. Novikov, P. A. Abramov, M. N. Sokolov and S. A. Adonin, *Chem. Eur. J.*, 2021, **27**, 9292-9294.
54. S. A. C. McDowell, *Chem. Phys. Lett.*, 2020, **742**, 137173.
55. M. Esrafili and P. Mousavian, *Molecules*, 2018, **23**, 2642.
56. G. Sánchez-Sanz and C. Trujillo, *J. Phys. Chem. A*, 2018, **122**, 1369-1377.
57. S. M. Cybulski and S. Scheiner, *J. Am. Chem. Soc.*, 1989, **111**, 23-31.
58. E. A. Hillenbrand and S. Scheiner, *J. Am. Chem. Soc.*, 1984, **106**, 6266-6273.
59. S. Scheiner, *Chem. Eur. J.*, 2016, **22**, 18850-18858.
60. M. A. A. Ibrahim, R. R. A. Saeed, M. N. I. Shehata, E. E. B. Mohamed, M. E. S. Soliman, J. H. Al-Fahemi, H. R. A. El-Mageed, M. N. Ahmed, A. M. Shawky and N. A. M. Moussa, *J. Mol. Struct.*, 2022, 133232.
61. M. A. A. Ibrahim, R. R. A. Saeed, M. N. I. Shehata, M. N. Ahmed, A. M. Shawky, M. M. Khowdiary, E. B. Elkaeed, M. E. S. Soliman and N. A. M. Moussa, *Int. J. Mol. Sci.*, 2022, **23**, 3114.
62. M. A. A. Ibrahim, A.-s. S. M. Rady, M. E. S. Soliman, M. F. Moustafa, H. R. A. El-Mageed and N. A. M. Moussa, *Struct. Chem.*, 2022, **33**, 9-21.
63. Y. Zhang and W. Wang, *J. Chem. Phys.*, 2020, **153**, 214302.
64. J. Echeverría, J. D. Velásquez and S. Alvarez, *Cryst. Growth Des.*, 2020, **20**, 7180-7187.
65. C. Wang, D. Danovich, S. Shaik, W. Wu and Y. Mo, *J. Comput. Chem.*, 2019, **40**, 1015-1022.
66. Y. Zhang and W. Wang, *Comput. Theor. Chem.*, 2022, **1213**, 113736.
67. F. Weinhold and R. A. Klein, *Angew. Chem. Int. Ed.*, 2014, **53**, 11214-11217.
68. F. Weinhold, *Inorg. Chem.*, 2018, **57**, 2035-2044.
69. L. Andreo, R. M. Gomila, E. Priola, A. Giordana, S. Pantaleone, E. Diana, G. Mahmoudi and A. Frontera, *Cryst. Growth Des.*, 2022, **22**, 6539-6544.

70. M. Calabrese, A. Pizzi, A. Daolio, A. Frontera and G. Resnati, *Chem. Commun.*, 2022, **58**, 9274-9277.
71. C. Loy, J. M. Holthoff, R. Weiss, S. M. Huber and S. V. Rosokha, *Chem. Sci.*, 2021, **12**, 8246-8251.
72. L. M. Azofra, J. Elguero and I. Alkorta, *J. Phys. Chem. A*, 2020, **124**, 2207-2214.
73. Í. Iribarren, M. M. Montero-Campillo, I. Alkorta, J. Elguero and D. Quiñonero, *Phys. Chem. Chem. Phys.*, 2019, **21**, 5796-5802.
74. A. Grabarz, M. Michalczyk, W. Zierkiewicz and S. Scheiner, *Molecules*, 2021, **26**, 2116.
75. G. Wang, Z. Chen, Z. Xu, J. Wang, Y. Yang, T. Cai, J. Shi and W. Zhu, *J. Phys. Chem. B*, 2016, **120**, 610-620.
76. D. Quinonero, I. Alkorta and J. Elguero, *Phys. Chem. Chem. Phys.*, 2016, **18**, 27939-27950.
77. R. Wysokiński, W. Zierkiewicz, M. Michalczyk, T. Maris and S. Scheiner, *Molecules*, 2022, **27**, 2144.
78. W. Zierkiewicz, M. Michalczyk, T. Maris, R. Wysokiński and S. Scheiner, *Chem. Commun.*, 2021, **57**, 13305-13308.
79. R. Wysokiński, *Phys. Chem. Chem. Phys.*, 2022, **24**, 12860-12869.
80. L. Chen, Q. Feng, C. Wang, S. Yin and Y. Mo, *J. Phys. Chem. A*, 2021, **125**, 10428-10438.
81. F. Yang, K. A. Behrend, H. Knorke, M. Rohdenburg, A. Charvat, C. Jenne, B. Abel and J. Warneke, *Angew. Chem. Int. Ed.*, 2021, **60**, 24910-24914.
82. J. M. Holthoff, E. Engelage, R. Weiss and S. M. Huber, *Angew. Chem. Int. Ed.*, 2020, **59**, 11150-11157.
83. D. Quiñonero, I. Alkorta and J. Elguero, *ChemPhysChem.*, 2020, **21**, 1597-1607.
84. R. Barbas, R. Prohens, A. Bauzá, A. Franconetti and A. Frontera, *Chem. Commun.*, 2019, **55**, 115-118.
85. I. Alkorta, I. Mata, E. Molins and E. Espinosa, *Chem. Eur. J.*, 2016, **22**, 9226-9234.
86. T. Niemann, P. Stange, A. Strate and R. Ludwig, *Phys. Chem. Chem. Phys.*, 2019, **21**, 8215-8220.
87. P. R. Horn, Y. Mao and M. Head-Gordon, *Phys. Chem. Chem. Phys.*, 2016, **18**, 23067-23079.

Table 1. Characteristics of Lewis base monomers, and the halogen-bonded complexes formed between their homonuclear π-clouds and ICCH.

	$V_{min,S}$ kcal/mol	$V_{min,Ax}$ kcal/mol	$-E_{int}$ kcal/mol	ES kcal/mol	R(I··mid) Å	ρ_{BCP} au	E2 kcal/mol	CT me
C_2H_2	-16.0	-20.2	3.01	-4.79	3.319	0.0106	2.5	11.9
C_2H_4	-15.8	-20.6	3.34	-5.48	3.317	0.0110	3.3	14.2
C_6H_6	-16.9	-17.0	3.87	-4.31	3.459	0.0082	1.4	9.6
C_2F_2	-1.8	-2.1	1.68	-2.38	3.336	0.0105	2.7	9.7
C_2F_4	+10.7	x	0.95	-0.62	3.371	0.0102	2.9	17.3
C_6F_6	+15.9	x	1.52	-1.11	3.483	0.0079	1.3	10.6

Table 2. SAPT decomposition of the interaction energy of each base with ICCH; all in kcal/mol.

	ES	EX	IND	DISP	TOT	%ES[a]
C_2H_2	-4.79	6.78	-1.71	-3.61	-3.33	47.4
C_2H_4	-5.48	7.94	-2.04	-4.09	-3.66	47.2
C_6H_6	-4.31	7.44	-1.67	-6.54	-5.08	34.4
C_2F_2	-2.38	5.33	-1.20	-3.37	-1.62	34.2
C_2F_4	-0.62	4.75	-1.15	-3.60	-0.62	11.5
C_6F_6	-1.11	6.00	-1.16	-6.08	-2.34	13.3

[a]ES/(ES+IND+DISP)

Table 3. Characteristics of Lewis base monomers, and the halogen-bonded complexes formed between their heteronuclear π-clouds and ICCH.

	$V_{min,S}$, kcal/mol	$V_{min,Ax}$, kcal/mol	$-E_{int}$, kcal/mol	ES kcal/mol	R(I··mid) Å	ρ_{BCP} au	E2 kcal/mol	CT me
F_2CO	x	x	x					
H_2CS	x	-2.0	x					
Me_2CS	x	-6.3	3.64	-4.74	3.413	0.0102	2.5	9.2
Me_2CTe	x	-6.1	4.00	-5.27	3.547	0.0095	3.2	15.1

Table 4. Characteristics of Lewis base monomers, and the halogen-bonded complexes formed between their N or P lone pairs and ICCH.

	$V_{min,S}$ kcal/mol	$V_{min,Ax}$ kcal/mol	$-E_{int}$ kcal/mol	ES kcal/mol	R(I··Z) Å	ρ_{BCP} au	E2 kcal/mol	CT me
NH_3	-40.1	-68.7	6.56	-11.49	2.978	0.0191	8.3	32.1
NCF	-29.6	-37.8	3.46	-5.18	3.082	0.0129	3.9	8.8
$NCNO_2$	-17.4	-21.9	2.17	-3.27	3.164	0.0110	2.8	4.5
NF_3	-3.9	-5.6	1.02	-1.51	3.260	0.0100	2.9	14.1
$N(NO_2)_3$	+4.0	+3.8	1.33	-0.94	3.243	0.0107	2.2	4.3
PF_3	+3.1	+3.1	1.12	-2.51	3.612	0.0097	4.5	34.2

Table 5. Characteristics of Lewis acid monomers, and the halogen-bonded complexes formed between their X atom and NH_3.

	$V_{max,S}$ kcal/mol	$-E_{int}$, kcal/mol	ES kcal/mol	R(X··N), Å	ρ_{BCP}, au	E2, kcal/mol	CT me
GeH_3I	+7.6	1.63	-3.65	3.320	0.0113	2.8	8.2
GeH_3Br	-0.4	0.44	-1.07	3.384	0.0080	1.3	2.7
GeH_3Cl	-7.1	x					
$GeMe_3Br$	-8.8	x					
$GeMe_3I$	-1.9	x					
C_6Me_5Br	+4.6	1.25	-3.00	3.161	0.0116	3.1	10.8
C_6Me_5Cl	+0.4	0.45	-1.42	3.150	0.0100	1.9	6.5

Table 6. SAPT decomposition of the interaction energy of various Lewis acids with indicated base; all in kcal/mol.

	ES	EX	IND	DISP	TOT	%ES
NH_3						
ICCH	-11.49	11.96	-3.66	-3.62	-6.82	61.2
ICH_3	-5.96	8.23	-2.11	-2.83	-2.66	54.7
$N(NO_2)_3$						
ICCH	-0.94	4.43	-0.82	-4.41	-1.74	15.2
ICH_3	-1.72	4.26	-0.49	-4.17	-2.12	27.0
$ClCH_3$	-1.64	2.80	-0.31	-2.78	-1.93	34.7
C_2H_4						
ICCH	-5.48	7.94	-2.04	-4.09	-3.66	47.2
ICH_3	-3.29	5.82	-1.04	-3.38	-1.89	42.7
C_2F_4						
ICCH	-0.62	4.75	-1.15	-3.60	-0.62	11.5
ICH_3	-1.53	4.57	-0.70	-3.43	-1.08	27.0
$ClCH_3$	-1.98	3.87	-0.47	-2.51	-1.09	39.9

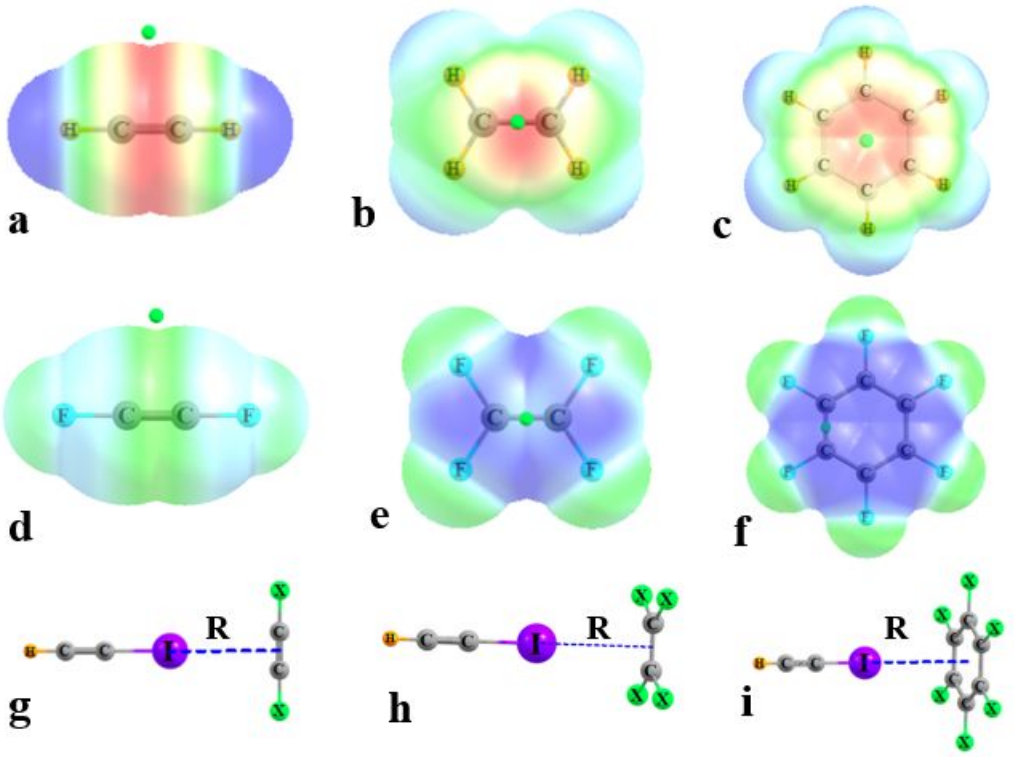

Fig 1. a-f) MEP lying above the plane of each molecule. Blue regions correspond to positive MEP (+20 kcal/mol), while negative is indicated by red (-20 kcal/mol), each drawn on surface corresponding to 1.5 x vdW radius. Small green ball indicates position of minimum. g-i) Geometries of optimized complexes with ICCH. R refers to distance between I and center of C-C bonds in g and h, and the center of the ring in i.

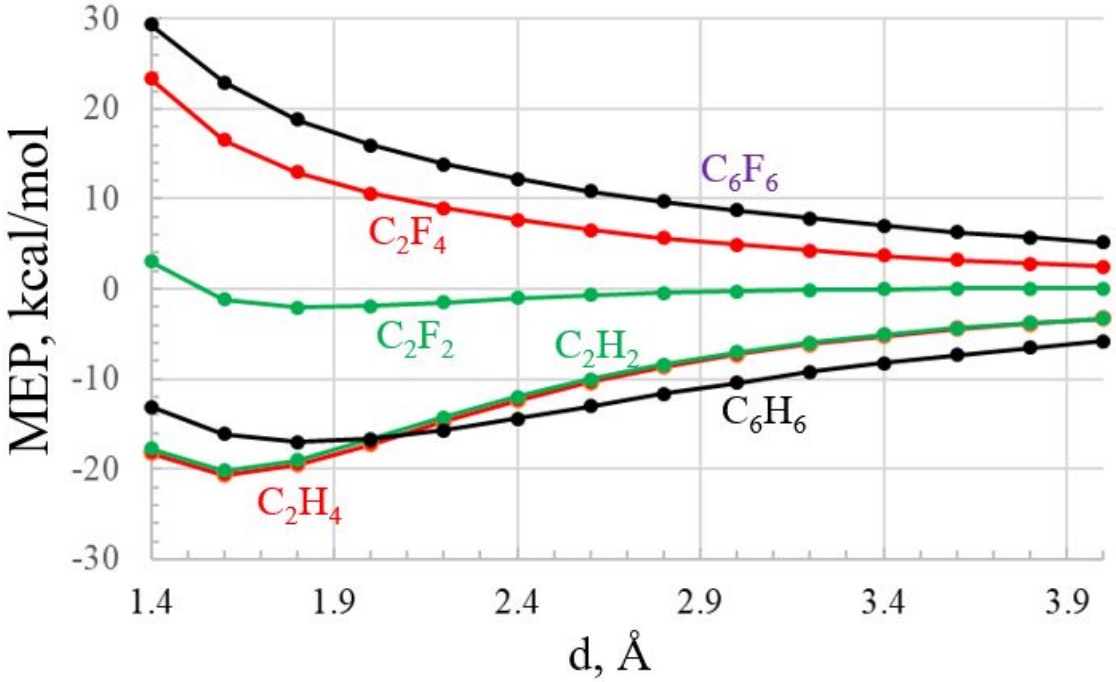

Fig 2. MEP evaluated at a distance d from the center of the C-C bond in the alkenes and alkynes, and from the center of the ring in C_6H_6 and C_6F_6.

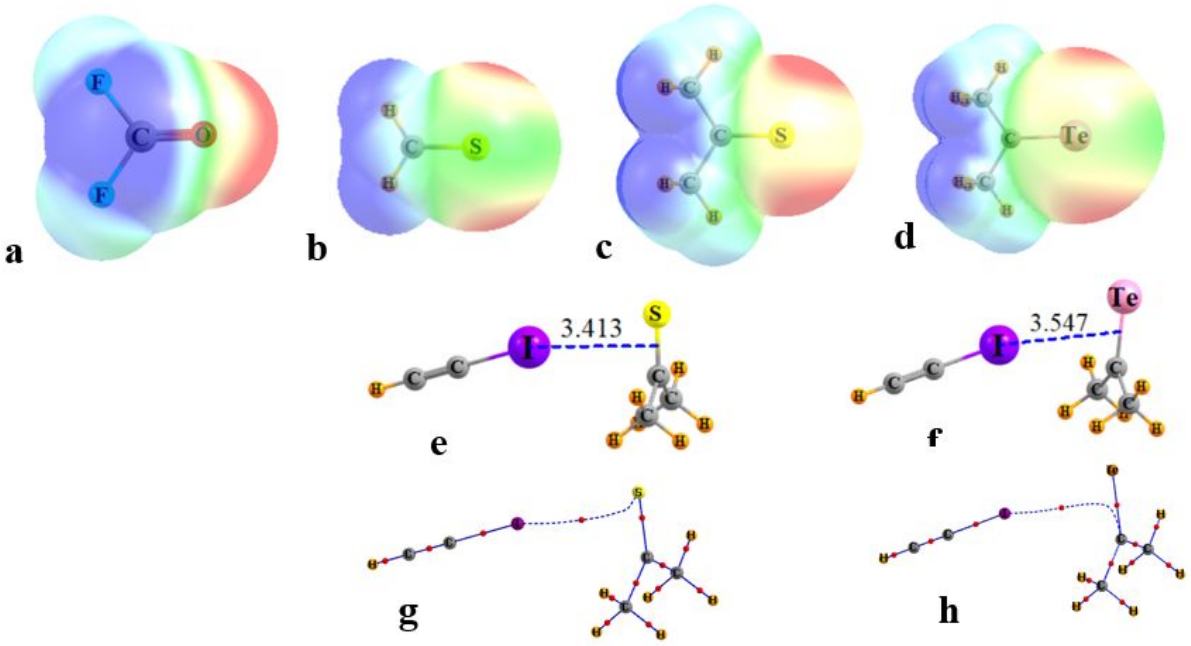

Fig 3. a-d MEP lying above the plane of each molecule. e,f) Geometries of optimized complexes with ICCH, with distance (Å) shown from I to center of C=Y bond. g,h) AIM molecular graphs of optimized geometries, with bond critical points indicated by small red balls.

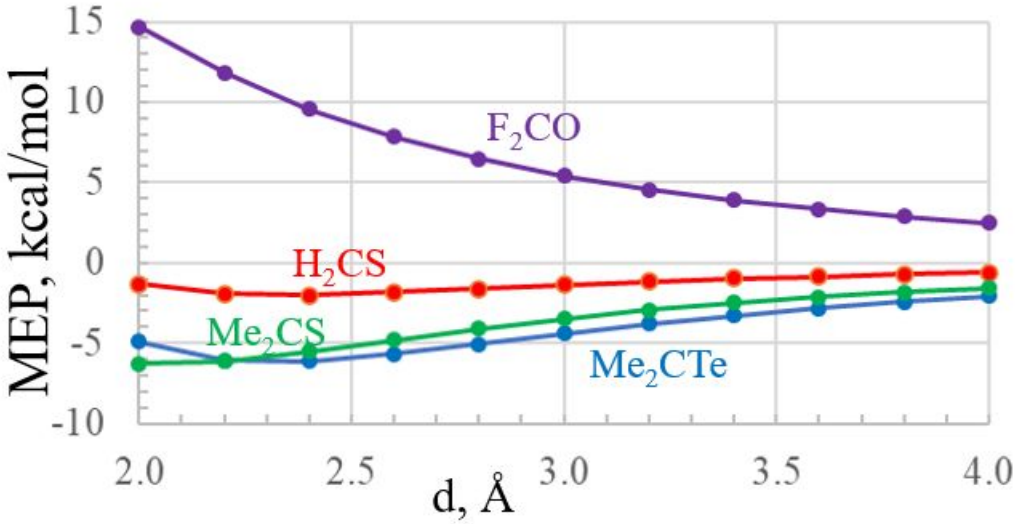

Fig 4. MEP evaluated at a distance d from the center of the C-Y bond, along a line perpendicular to the molecule.

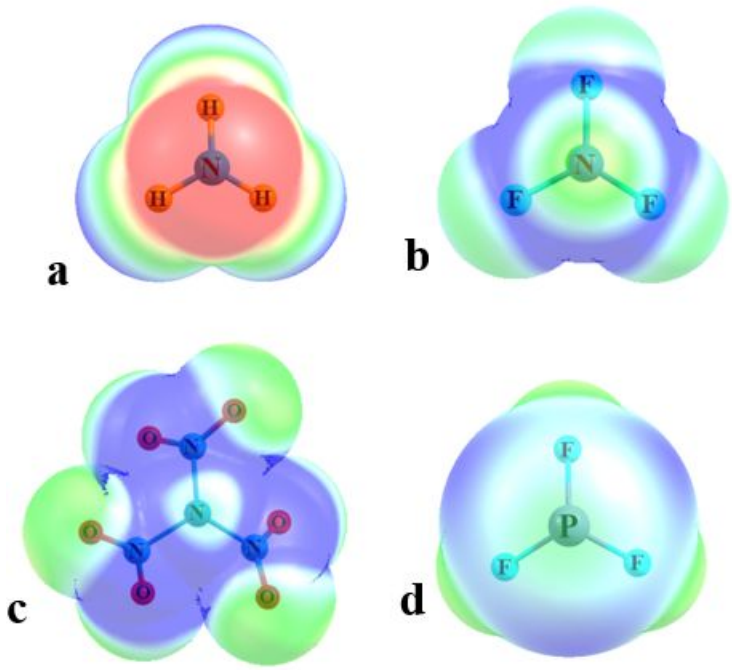

Fig 5. MEP lying above the plane of a) NH_3, b) NF_3, c) $N(NH_2)_3$, and d) PF_3.

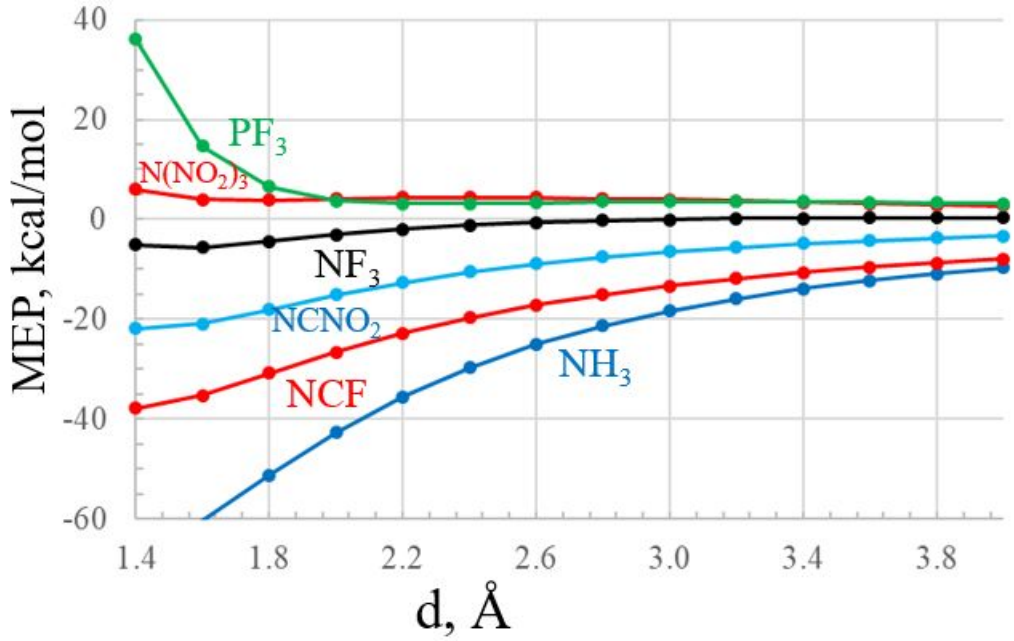

Fig 6. MEP evaluated at a distance d from the central N or P atom, along either the C_3 or C-N lone pair axis.

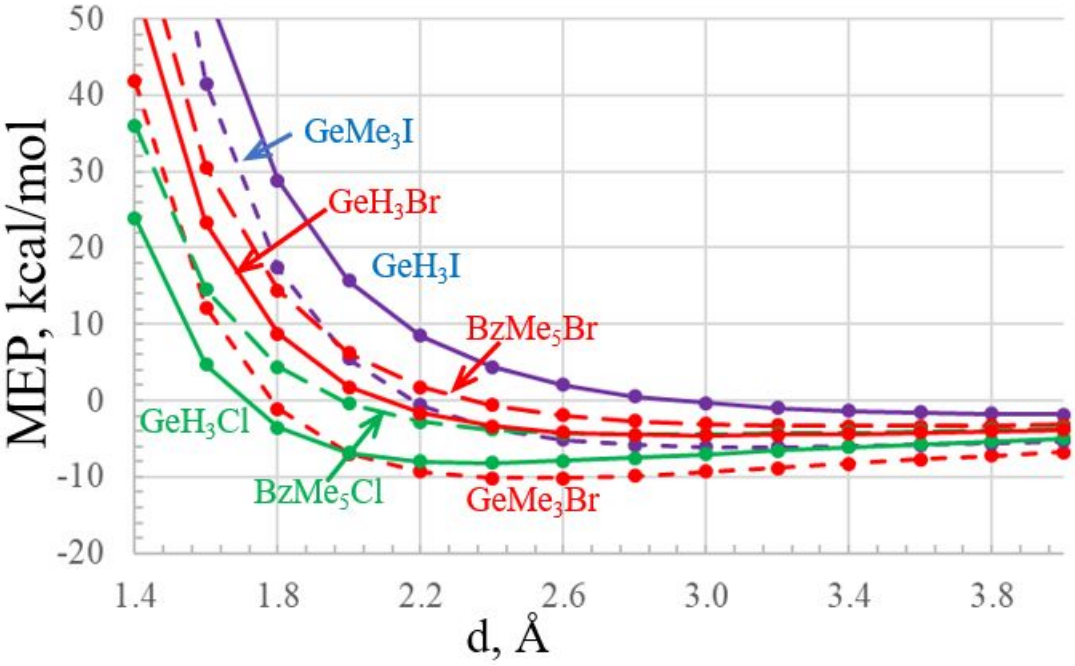

Fig 7. MEP evaluated at a distance d from the X atom, along the extension of the T-X covalent bond.

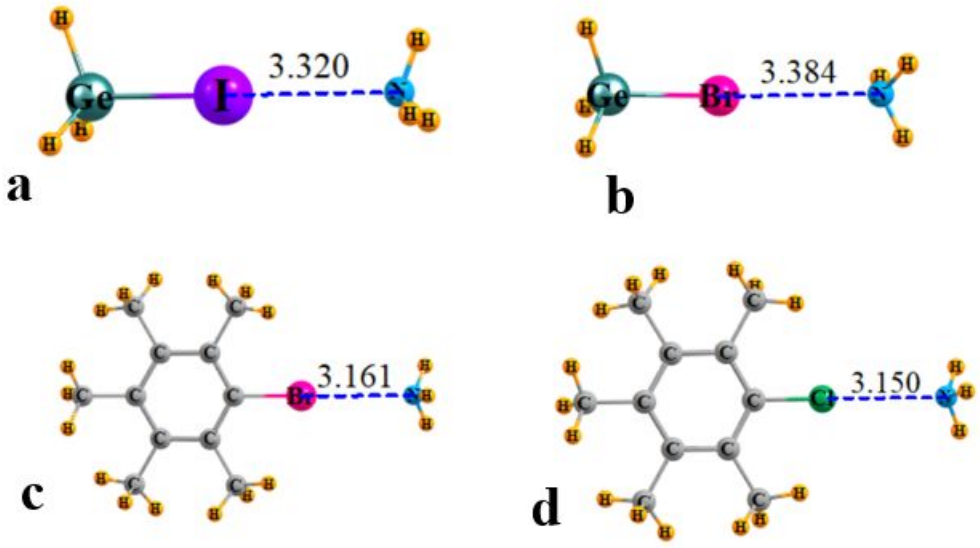

Fig 8. Geometries of optimized complexes with NH_3, X··N distance in Å.